Editors' Suggestion

Dynamics of three-dimensional turbulence from Navier-Stokes equations

Katepalli R. Sreenivasan[1,*] and Victor Yakhot[2,1,†]

[1]*Department of Mechanical and Aerospace Engineering, Courant Institute of Mathematical Sciences, and Department of Physics, New York University, New York 11201, USA*

[2]*Department of Mechanical Engineering, Boston University, Boston, Massachusetts 02215, USA*

(Received 11 June 2021; accepted 15 September 2021; published 15 October 2021)

In statistically homogeneous and isotropic turbulence, the average value of the velocity increment $\delta_r u = u(x+r) - u(x)$, where x and $x+r$ are two positions in the flow and u is the velocity in the direction of the separation distance r, is identically zero, and so to characterize the dynamics one often uses the Reynolds number based on $\sqrt{\langle(\delta_r u)^2\rangle}$, which acts as the coupling constant for scale-to-scale interactions. This description can be generalized by introducing structure functions of order n, $S_n = \langle(\delta_r u)^n\rangle$, which allow one to probe velocity increments including rare and extreme events, by considering $\delta_r u(n) = O(S_n^{1/n})$ for large and small n. If $S_n \propto r^{\zeta_n}$, the theory for the anomalous exponents ζ_n in the entire allowable interval $-1 < n < \infty$ is one of the long-standing challenges in turbulence (one takes absolute values of $\delta_r u$ for negative n), usually attacked by various qualitative cascade models. We accomplish two major tasks here. First, we show that the turbulent microscale Reynolds number R_λ^T (based on a suitably defined turbulent viscosity) is 8.8 in the inertial range with anomalous scaling, when the standard microscale Reynolds number R_λ (defined using normal viscosity) exceeds that same number (which in practice could be by a large factor). When the normal and turbulent microscale Reynolds numbers become equal to or fall below 8.8, the anomaly disappears in favor of Gaussian statistics. Conversely, if one starts with a Gaussian state and increases R_λ beyond 8.8, one ushers in the anomalous scaling; the inference is that $R_\lambda^T \approx 8.8$ and remains constant at that value with further increase in R_λ. Second, we derive expressions for the anomalous scaling exponents of structure functions and moments of spatial derivatives, by analyzing the Navier-Stokes equations in the form developed by Hopf. We present a novel procedure to close the Hopf equation, resulting in expressions for ζ_n in the entire range of allowable moment order n, and demonstrate that accounting for the temporal dynamics changes the scaling from normal to anomalous. For large n, the theory predicts the saturation of ζ_n with n, leading to several inferences, two among which are (a) the smallest length scale $\eta_n = L\mathrm{Re}^{-1} \ll L\mathrm{Re}^{-3/4}$, where Re is the large-scale Reynolds number, and (b) that velocity excursions across even the smallest length scales can sometimes be as large as the large-scale velocity itself. Theoretical predictions for each of these aspects are shown to be in excellent quantitative agreement with available experimental and numerical data.

DOI: 10.1103/PhysRevFluids.6.104604

I. INTRODUCTION

Turbulent flows are everywhere. Without them life on Earth would be impossible, for they are responsible for the life-sustaining heat and mass transfer. Indeed, it is easy to estimate that, due to

*krs3@nyu.edu
†vy@bu.edu

absorbed solar radiation, one summer without turbulence would be long enough to boil a four-meter layer of ocean water. Also, it is responsible for the temperature control and ventilation in various modern engineering applications, such as data centers, transportation, and chemical technology—in short, for all aspects of our life.

Turbulent flows differ by geometry, smoothness or otherwise of the boundaries, physical noise, details of transitions from laminar to turbulent states, etc. Not surprisingly, they are characterized by transitional Reynolds numbers varying over an enormously wide range. For example, depending on the quality of walls and the quietness of the oncoming stream, the transition Reynolds number in a channel flow can vary over two orders of magnitude. But the excited length scales in turbulence, dependent on the Reynolds number, are very wide at high Reynolds numbers, and so one can ask a logical question: do the small-scale velocity fluctuations at high Reynolds number "remember" geometric and other features of their laminar precursors? If they do, different flows must be described by different turbulence theories, involving detailed information on laminar-turbulent transition as well as boundary conditions, which seems to be a mission impossible. If they do not, one can hope for the universality classes and universal theory, qualitatively similar to critical phenomena. Addressing this avenue is the primary purpose of this paper.

To describe fluid motion, Euler [1] derived his field equations for an ideal (inviscid) fluid which, among other concepts, contained the Bernoulli equation obtained almost 20 years earlier. Later, Navier [2] and Stokes [3] came up with the equations for the motion of viscous fluids which, combined with modern numerical and computational methods, have revolutionized modern fluid dynamics. These achievements have solved the problem of all laminar (or regular) flows, including time-dependent ones such as flows past oscillating plates, bluff bodies, etc.

Transition to turbulence was experimentally discovered and studied by Reynolds [4], who introduced his famous decomposition of the velocity field into its regular and stochastic components. This work initiated the field of statistical hydrodynamics based on the generally accepted belief that both laminar and turbulent flows can be accurately described by the Navier-Stokes (NS) equations. This factor led in due course to the formulation of various field-theoretical approaches such as Wyld's renormalized expansions in powers of Reynolds number [5,6], Kraichnan's direct interaction approximation (DIA) and lagrangian history direct interaction approximation (LHDIA) approximations [7,8], Orszag's Eddy Damped Quasi-Normal Markovian approach [9], etc. They have had considerable successes in the derivation of large-scale turbulence models widely used in engineering computations of flows in complex geometries [10–15] but have failed in the *a priori* prediction of small-scale features dominated by powerful intermittent structures, which occupy an increasingly smaller fraction of volume with increasing Reynolds number [16] and are responsible for the ever-changing intricate images that have fascinated and inspired humans for hundreds of years.

The theory of critical phenomena, renormalization group, and the ϵ expansion are among the most remarkable achievements of theoretical physics of the 20th century—perhaps even as a philosophical paradigm [17] (see, especially, articles by Kadanoff and Lubin in Vol. 5 and those by Wilson and Wegner in Vol. 6 of Ref. [17]). The theory is thought to be still incomplete, since it is based on approximations that do not solve the three-dimensional (3D) Ising model exactly [18], but the large-scale features of critical systems are well understood in terms of a single divergent length scale $\xi \propto |T - T_{cr}|^{-\nu}$, where $T - T_{cr}$ is the distance from the critical temperature T_{cr} and ν is a universal exponent. However, the small-scale details of the model are unknown, as the "scaling hypothesis," based on correlation length $\xi \to \infty$, is definitely not valid for scales of the order of the mean free path. But what makes this approach successful is that such small scales do not play a significant role at the critical point.

The problem of hydrodynamic turbulence at large Reynolds numbers is very different, as it appears that all flow scales of the continuum—large, intermediate, and small—are dynamically important, and that this dynamics is hard to extract from the NS equations, which are believed to apply to a large variety of conditions, including those near the critical point in phase transitions (even though they can be derived directly from microscopic molecular dynamics only for rarefied gases for scales much larger than the mean free path). These equations describe velocity fluctuations

generated at the large scale L and dissipated on a scale η whose ratio to L becomes vanishingly small as an inverse power of the Reynolds number. No energy is lost in this nonlinear inviscid process of the so-called inertial-range energy transfer which requires strong interactions between fluctuations on different length scales, very different from detailed balancing that is characteristic of microscopic reversibility. The process of formation of small-scale fluctuations out of large scales, often called the energy cascade, was introduced as an explicit notion in Ref. [19] but implied already in Kolmogorov's earlier work [20]. Qualitatively the cascade resembles the process leading to the formation of high-energy fractions formed in hadron collisions, where it is responsible for anomalous scaling exponents characterizing the collision process [21].

For many years, due to the lack of sufficiently accurate and extensive experimental data, the existence of anomalous scaling in high-Reynolds-number turbulence was set aside from serious consideration. That era is thankfully over, and the existence of anomalous scaling and its possible universality, i.e., independence of scaling exponents on the nature of a flow, has been established as a result of many years of hard work by several groups (see, e.g., Refs. [22–28]).

In this paper we consider an infinitely extended fluid stirred (or forced) by a random force at the scale L. We first show that as $r/L \to \infty$, the large-scale flow that is generated is Gaussian in accordance with the central limit theorem and the dynamic renormalization group worked out by Forster, Nelson, and Stephen [29]. Due to the specific nonlinearity of the NS equations, the small-scale asymptotics $r/L \to 0$ corresponds to strong coupling, which makes the turbulence problem very hard. Here, we first recall a previously derived expression [12,30] for the effective viscosity in the inertial range, and note that the Reynolds number based on that effective viscosity assumes a universal value of about 8.8. We next consider the anomalous scaling of structure functions in the inertial range and develop a theory based on the Hopf formulation [31] of the NS equations and provide an explicit expression for anomalous scaling exponents ζ_n for structure functions in the entire range $-1 < n < \infty$; structure functions are moments of velocity increments $\delta_r u = u(x + r) - u(x)$ and the scaling exponents ζ_n are defined by the expected relation $\langle(\delta_r u)^n\rangle \propto r^{\zeta_n}$ in the range $\eta \ll r \ll L$. We take recourse to Polyakov's application of point splitting for the Burgers equation that is driven by a random force [32], generalized to the three-dimensional NS equations in Refs. [33–36]. A crucial feature in this paper is that we do not use any specific model for pressure-velocity correlations. Earlier, Yakhot [33,35,36] had used specific models for pressure-velocity correlations to the same end. These models were assessed in Ref. [37] and also in Ref. [38], where the Hopf equation was combined with the Bernoulli equation as an input model for pressure-velocity correlation. In a third aspect of the paper, we note the effective analogy to laminar-turbulent transition that has been observed in direct numerical simulation (DNS) to occur at a microscale Reynolds number of about 9, not different from 8.8 above. We discuss a possible connection of this result to the two aspects just mentioned.

Since the paper touches on a number of interrelated topics, it is useful to provide a quick roadmap here. The first principal goal for the paper is to show that the turbulent microscale Reynolds number R_λ^T (based on a well-defined turbulent viscosity) is 8.8 in the inertial range with anomalous scaling, when the standard microscale Reynolds number R_λ (defined using normal viscosity) exceeds that same number (perhaps manyfold in practice). When the normal and turbulent microscale Reynolds numbers fall below 8.8, the anomaly disappears in favor of Gaussian statistics. Conversely, if one starts with a Gaussian state and increases R_λ beyond 8.8, one ushers in the anomalous scaling; the inference is that $R_\lambda^T \approx 8.8$ and remains constant at that value with further increase in R_λ. That is, there exists a critical Reynolds number of 8.8 which separates the Gaussian state from the multiscaling regime. This part of the work is described primarily in Secs. II, III, and VII C. In Sec. II, we show using the Fourier space representation that the NS equations driven by a random force at the wavenumber $\Lambda = \frac{2\pi}{L}$ obey Gaussian statistics in the limit of the wavenumber $k/\Lambda \to 0$, in accordance with Ref. [29]. Section III shows that in the inviscid inertial range there is a scale-independent effective or turbulent Reynolds number at which transition from the Gaussian state to the inertial range takes place. In Sec. VII C, we recapitulate recent numerical work that describes the transition from the Gaussian state to the multiscaling state.

Our second principal goal is to predict, without the use of modeling, the scaling exponents in the anomalous multiscaling state. This is the work described in Secs. IV–VII. In Sec. IV, the Hopf equations are derived and the point-splitting procedure is presented as a step towards closing the Hopf equation. Section V evaluates the coarse-grained NS equations for pressure contributions and obtains scaling exponents of structure functions of all orders. We show in Sec. VI that ignoring the time derivative in the NS equations leads to the Kolmogorov scaling $\zeta_{2n} = 2n/3$, and that one obtains anomalous scaling when both spatial and temporal dependencies are included.

These pieces of work essentially bring to some conclusion the program of understanding large and small scales of homogenous and isotropic turbulence. The predictions of the theory are compared with experiments in Sec. VII, and excellent agreement is achieved. Finally, Sec. VIII is devoted to a brief recapitulation of results and conclusions.

II. THE MODEL: LARGE-SCALE GAUSSIAN STATISTICS

Flow of Newtonian fluids can be described by the NS equations subject to boundary and initial conditions (with the density ρ set to unity without loss of generality),

$$\partial_t \mathbf{u} + \mathbf{u}\cdot\nabla\mathbf{u} = -\nabla p + \nu\nabla^2\mathbf{u} + \mathbf{f}, \tag{1}$$

and the incompressibility condition given by $\nabla\cdot\mathbf{u} = 0$. The random white-in-time Gaussian forcing $\mathbf{f}$ is defined by the correlation function [12,29]

$$\langle f_i(\mathbf{k},\omega) f_j(\mathbf{k}',\omega')\rangle = (2\pi)^{d+1} D_0(k) P_{ij}(\mathbf{k})\delta(\hat{k}+\hat{k}'), \tag{2}$$

where the four-vector $\hat{k} = (\mathbf{k},\omega)$ and the projection operator is given by $P_{ij}(\mathbf{k}) = \delta_{ij} - \frac{k_i k_j}{k^2}$. Here we are interested in the case $D_0(k) \neq 0$ only close to κ. Taking the Fourier transform of (1) as

$$u_l(\mathbf{k},\omega) = G^0 f_l(\mathbf{k},\omega) - \frac{i}{2} G^0 \mathcal{P}_{lmn} \int u_m(\mathbf{q},\Omega) u_n(\mathbf{k}-\mathbf{q},\omega-\Omega) d\mathbf{q} d\Omega, \tag{3}$$

where $G^0 = (-i\omega + \nu k^2)^{-1}$, $\mathcal{P}_{lmn}(\mathbf{k}) = k_n P_{lm}(\mathbf{k}) + k_m P_{ln}(\mathbf{k})$, we introduce the zero-order solution $\mathbf{u}_0 = G^0\mathbf{f} \propto k\sqrt{D_0}$, so that $\mathbf{u} = G^0\mathbf{f} + \mathbf{v}$, and derive the equation for the perturbation velocity $\mathbf{v}$ to be

$$\begin{aligned} v_l(\hat{k}) = &-\frac{i}{2} G^0(\hat{k}) \mathcal{P}_{lmn}(\mathbf{k}) \int v_m(\hat{q}) v_n(\hat{k}-\hat{q}) d\hat{q} - \frac{i}{2} G^0(\hat{k}) \mathcal{P}_{lmn}(\mathbf{k}) \int [v_m(\hat{q}) G^0(\hat{k}-\hat{q}) f_n(\hat{k}-\hat{q}) \\ &+ G^0(\hat{q}) f_m(\hat{q}) v_n(\hat{k}-\hat{q})] d\hat{q} - \frac{i}{2} G^0(\hat{k}) \mathcal{P}_{lmn}(\mathbf{k}) \int G^0(\hat{q}) f_m(\hat{q}) G^0(\hat{k}-\hat{q}) f_n(\hat{k}-\hat{q}) d\hat{q}. \end{aligned} \tag{4}$$

Because of the nonlinearity of the NS equations, the modes away from the large-scale range $k \to 0$, where the forcing $\mathbf{f}(k) = 0$, are populated by the effective forcing $\mathbf{F}$ [12,29] as

$$\langle F_i(\mathbf{k}) F_j(\mathbf{k}')\rangle \approx 2 D_L k^2 P_{ij}(\mathbf{k})\delta(\mathbf{k}+\mathbf{k}') + O(k^4), \tag{5}$$

where (see Ref. [30])

$$D_L = (2\pi)^{d+1} D_0 \frac{0.155}{\Lambda^5}, \tag{6}$$

which is small in the limit $\frac{k}{\Lambda}\sqrt{\frac{D_0}{D_L}} \to 0$. In this scale range of weak coupling $|F(k)|^2 \propto k^2 D_0 \to 0$, the low-order perturbation expansion is accurate, and the flow is in "thermodynamic equilibrium," stabilized by a small *induced* viscosity $\nu_{eff} = \nu_0 + \delta\nu$ where ν_0 is the bare viscosity and $\delta\nu \propto D_L$. In an infinitely extended fluid satisfying the limiting condition $k^2 D_0 \to 0$, the flow that is generated is Gaussian by virtue of the central limit theorem and dynamic renormalization group [12,29,30], independent of the statistics of the force $\mathbf{f}$ introduced earlier.

To conclude this section devoted to the large-scale behavior at $k \ll \Lambda$, we note that in the strong turbulence range $k \gg \Lambda$, the induced forcing evaluated in the low-order approximation is $\langle F^2\rangle \propto$

k^{-3}. This model was introduced in Ref. [39]. It is clear that the entire turbulence production in the force-driven turbulence has a logarithmic divergence, compensated by the infrared range and higher nonlinearities that are not directly relevant in our considerations.

III. THE MODEL: SMALL-SCALE ASYMPTOTICS AND THE CRITICAL REYNOLDS NUMBER

In the large-wavenumber regime often referred to as the ultraviolet regime, $k \gg \Lambda$ with $k^2 D_0 \to \infty$, the dynamics are far from equilibrium and perturbation expansions break down. In this range, the flow is driven by an effective forcing and the energy is drained out by viscosity in the dissipation range. While the induced field is weak in the weak-coupling range $k \to 0$, it is strong in the limit $k/\Lambda \to \infty$ and is responsible for various nonlinear effects considered below. One can attempt to extend Wyld's expansion into this range but the task is difficult because such expansions are haunted by infrared divergences [7,8,29].

In summary, at large scales $k \ll \Lambda$, the velocity fluctuations in the flows driven by the forcing centered at $\Lambda = \frac{2\pi}{L}$ are Gaussian, justifying various one-loop approximations to renormalized perturbation expansions. The modes with $k \gg \Lambda$ are populated by strong nonlinearity, and the proper matching between viscous and inertial range effects becomes a dominant mechanism responsible for anomalous scaling and strong departures from Gaussian statistics.

We stress the lack of small parameter in the inertial range by the following argument [40]. For the velocity increment u_r in the inertial range where dissipation by the molecular viscosity is negligible, the effective or turbulent viscosity governing the dynamics of inertial scales ($L \gg r \gg \eta$) is given by $\nu_T \approx r u_r$; here u_r is a velocity characteristic of scale r, say, $[(u(x+r) - u(x))^2]^{1/2}$. In this case, the dimensionless coupling constant is the Reynolds number,

$$\mathrm{Re}(u_r) = \frac{r u_r}{\nu_T} = \mathrm{const} = O(1), \tag{7}$$

which is not small anywhere in the inertial range. Using the dynamic renormalization group, one derives the expression for turbulent viscosity as

$$\nu_T \equiv \nu(\Lambda) \approx 0.084 \frac{K^2}{\varepsilon}, \quad 10\nu^2(\Lambda) \times \Lambda^2 = K^2, \tag{8}$$

where $K \approx u_r^2/2$ is the kinetic energy of the turbulent motion on the inertial scales $r \leqslant L$, and ε is the mean rate of kinetic energy dissipation [12,30]. Landau and Lifshitz [40] (and others) have shown that the turbulent viscosity is $\nu_T(r) \propto r u_r$ given by (7) above.

An important point needs to be made. Relations (8) have been derived by the small-scale elimination from the interval $\eta < r < L$ and, therefore, give effective viscosity acting on large-scale fluctuations $k < \frac{2\pi}{r}$. Further, the effective Reynolds number of single-scale to multiscaling transition, based on the Taylor scale and turbulent parameters,

$$R_{\lambda,r} = 2K\sqrt{\frac{5}{3\varepsilon\nu(\Lambda)}} = 2\sqrt{\frac{5}{3 \times 0.084}} \approx 8.8, \tag{9}$$

is scale independent in the inertial range and is very close to the Reynolds number of transition from the Gaussian to the anomalous regime of the velocity field [41,42].

As an aside, this simple relation (9), combined with the definition of turbulent viscosity $\nu_T \propto \frac{\langle (\delta_r u)^4 \rangle}{\varepsilon}$, valid in homogeneously or smoothly excited flows, gives

$$\langle (\delta_r u)^3 \rangle \propto \varepsilon r, \tag{10}$$

which resembles the celebrated Kolmogorov relation for velocity increments in the inertial range of homogeneous and isotropic turbulence. Thus, the constant energy flux from large to small scales in turbulence makes all scales dynamically relevant, which leads to a gross violation of the scaling hypothesis in critical phenomena. This is the main reason for the failure of field-theoretical methods

like Wyld's expansion [5], Kraichnan's DIA and LHDIA [7,8], and others (see, for example, Ref. [6]).

It appears from this discussion that the infrared limit can be understood by the perturbation theory, so our goal in the next section is to develop the theory in the strong-coupling ultraviolet range, where $k > \Lambda$ and $k^2 D_0 \to \infty$.

IV. HOPF EQUATION, POINT SPLITTING, AND THE SCALING EXPONENTS

A. The Hopf equation

As was shown by Kolmogorov [43] in the high-Reynolds-number limit, the third-order structure function $S_3(r) = -\frac{4}{5}\varepsilon r$ in the inertial range of isotropic and homogeneous turbulence. This is the celebrated 4/5 law. Our goal is to discuss all even moments $S_{2n} = \langle (u(x+r) - u(x))^{2n} \rangle$ and their scaling exponents ζ_{2n} where $S_{2n} \propto r^{\zeta_{2n}}$. As already mentioned a large body of experimental work [24] has demonstrated that ζ_{2n} are different from Kolmogorov's normal scaling theory, $S_{2n}(r) \propto r^{2n\zeta}$, where the local velocity increment $[S_{2n}(r)]^{(1/2n)} \propto r^{\zeta}$ [20]. The problem of determining ζ_{2n}, if they are different from $2n\zeta$, is important because the high-order exponents relate to large excursions or the tails of the distribution of $\delta_r u$. We will consider some specific implications of this feature in Sec. VI.

We address the problem of determining ζ_{2n} using Hopf equation [31], adopting the approach used by Polyakov [32] for the description of the Burgers equation driven by a random force, later generalized in Refs. [13,15] to the case of 3D Navier-Stokes turbulence in the evaluation of velocity increments $\mathbf{U} \equiv \delta_{\mathbf{r}}\mathbf{u} = \mathbf{u}(\mathbf{x}+\mathbf{r}) - \mathbf{u}(\mathbf{x})$; see also Refs. [34,38]. We will show that, due to large nonlinearity, the probability of large-amplitude and rare fluctuations is much larger than that for the Gaussian determined by the second moment. It has been known for some time that the volume fraction occupied by these very local events, and thus the total expectation value of these events, is small [16].

The origins of the Hopf equation for the generating function $Z = \langle e^{(\boldsymbol{\lambda}.\boldsymbol{U})} \rangle$ goes back to Ref. [31]. The relevant equation for the generating function becomes

$$\frac{\partial Z}{\partial t} + \frac{\partial^2 Z}{\partial \lambda_\mu \partial r_\mu} = I_f + I_p + D, \tag{11}$$

$$I_f = \langle \boldsymbol{\lambda} \cdot \nabla \mathbf{f} e^{\lambda \cdot u_r} \rangle, \tag{12}$$

$$I_p = -\boldsymbol{\lambda} \cdot \langle e^{\lambda \cdot u_r} [\nabla_2 p(x_2) - \nabla_1 p(x_1)] \rangle, \tag{13}$$

and

$$D = \nu_0 \boldsymbol{\lambda} \cdot \left\langle \left[\nabla_2^2 v(x_2) - \nabla_1^2 v(x_1) \right] e^{\lambda \cdot u_r} \right\rangle. \tag{14}$$

The main difficulty in solving this equation is that it is not closed because of the dissipation and pressure terms (for a more detailed discussion, see Ref. [6]). A proper solution requires additional information to be gained from the NS equations themselves. In the inertial range where $\nu_0 \to 0$ and $r = |x_1 - x_2| \gg \eta$, the dissipation contribution $D = 0$. This is not so in the theoretically harder limit $r \approx \eta$ or $x_1 \to x_2$, which is important for closing the equation.

In the rest of the paper we define $S_{m,n} = \langle (\delta_r u)^m (\delta_r v)^n \rangle$, where u and v are velocity fluctuations in the direction of the separation and perpendicular to it, respectively. If n is zero, as is often the case below, it is not always mentioned explicitly for brevity. By symmetry, v is the same in any direction perpendicular to r. The equations for even-order moments [12,13,15] are

$$\frac{\partial S_{2n,0}}{\partial r} + \frac{d-1}{r} S_{2n,0} = \mathcal{P}\left[1 - \cos\left(\frac{r}{L}\right)\right] \alpha_{n,d} S_{2n-3,0} - (2n-1)\langle \delta_r(\partial_x p) \times (\delta_r u)^{2n-2} \rangle + \nu(2n-1)\langle \delta_r \hat{a} (\delta_r u)^{2n-2} \rangle, \tag{15}$$

where $\alpha_{n,d} = 2(2n-1)(2n-2)/d$, d being the dimensionality of the fluid system. By energy conservation, we have $\mathcal{P} = \varepsilon$; $\hat{a}$ is the Lagrangian acceleration of the fluid particle.

In particular, the last term in the above equation with $\delta_r \hat{a} = \hat{a}(x+r) - \hat{a}(x)$ is unknown and has to be treated properly. In the inertial range, for which $\nu \to 0$, $r \gg \eta$, and $\frac{r}{L} \to 0$, and the forcing term is zero; the implication is that the dissipation contribution is given by $\nu\langle \delta_r \hat{a} (\delta_r u)^{2n-2}\rangle = 0$. Thus,

$$\frac{\partial S_{2n,0}}{\partial r} + \frac{d-1}{r} S_{2n,0} - \frac{(d-1)(2n-1)}{r} S_{2n-2,2} = -(2n-1)\langle \delta_r(\partial_x p) \times (\delta_r u)^{2n-2}\rangle \tag{16}$$

and we can use the unsteady Bernoulli equation

$$-\frac{\partial p}{\partial x} = \frac{\partial v_x}{\partial t} + \frac{1}{2}\frac{\partial v_x^2}{\partial x} + v_y \frac{\partial v_x}{\partial y} + v_z \frac{\partial v_x}{\partial z}. \tag{17}$$

Upon substituting (17) in (16), the pressure contribution in the incompressible case disappears and one recovers the well-known results for $S_{3,0}(r)$ and $S_{1,2}$ as

$$\frac{\partial S_{3,0}}{\partial r} + \frac{d-1}{r} S_{3,0} - 2\frac{d-1}{r} S_{1,2} = -(1)^d \frac{4}{d}\mathcal{P}, \tag{18}$$

$$S_{3,0} = (-1)^d \frac{12}{d(d+2)} \mathcal{P} r, \tag{19}$$

and

$$\frac{1}{r^{d+1}} \frac{d}{dr} r^{d+1} S_{1,2} = (-1)^d \frac{4}{d}\mathcal{P}. \tag{20}$$

These relations are exact in the limit $\nu \to 0$ and yield for $d = 3$

$$\zeta_{2,0} = \zeta_{0,2}, \qquad \zeta_{3,0} = \zeta_{1,2}, \tag{21}$$

in addition to Kolmogorov's celebrated 4/5 law [43] and the relation $S_{3,0}/S_{1,2} = 3$.

B. Viscous effects, point splitting, and matching condition

Equation (15) contains both pressure and dissipation contributions and is not closed for general n. As we have shown, the dissipation contribution is small in the inertial range and can be neglected, resulting in Eq. (16). However, the pressure terms contain both derivatives and differences over r, which one needs to obtain by asymptotic matching of structure functions from inertial and dissipation ranges, leading to important dynamic consequences, as shown below (see also Ref. [15]).

As discussed in Ref. [40], if $\delta_\eta u \approx u(x+\eta) - u(x)$, the dissipation scale η is defined by the condition $\mathrm{Re}_\eta = O(1) = \eta(\delta_\eta u)/\nu$, so that $\eta = O(\nu/(\delta_\eta u))$. This simple algebra can be used to express spatial derivatives as

$$\partial_x u \approx (\delta_\eta u)^2/\nu. \tag{22}$$

This is the so-called point-splitting procedure. It follows that

$$\left(\frac{L}{u_0}\right)^{2n} \left\langle \left(\frac{\partial u}{\partial x}\right)^{2n} \right\rangle = \mathrm{Re}^{2n} \left(\frac{\eta_{4n}}{L}\right)^{\zeta_{4n}} \equiv \mathrm{Re}^{\rho_{2n}}, \tag{23}$$

where $\mathrm{Re} = u_0 L/\nu$, where u_0 is a large-scale property such as its root-mean-square value. We also get

$$\frac{L^n}{u_0^{3n}} \langle \varepsilon^n \rangle = \mathrm{Re}^n \frac{\langle (\delta_\eta u)^{4n}\rangle}{{u_0}^{4n}} = \mathrm{Re}^n S_{4n}(\eta_{4n}) = \mathrm{Re}^n \left(\frac{\eta_{4n}}{L}\right)^{\zeta_{4n}} \equiv \mathrm{Re}^{d_n}, \tag{24}$$

where the scaling exponents d_n and ρ_n are yet to be derived from an *a priori* theory. By applying the point-splitting procedure mentioned above (see Ref. [36]), we have

$$\frac{S_{2n}(\eta_{2n})}{\eta_{2n}} \approx \frac{S_{2n+1}(\eta_{2n})}{\nu}, \tag{25}$$

leading to

$$\frac{\eta_n}{L} = \mathrm{Re}^{\frac{1}{\zeta_n - \zeta_{n+1} - 1}}. \tag{26}$$

We also have two important additional relations,

$$\rho_n = n + \frac{\zeta_{2n}}{\zeta_{2n} - \zeta_{2n+1} - 1} \tag{27}$$

and

$$d_n = n + \frac{\zeta_{4n}}{\zeta_{4n} - \zeta_{4n+1} - 1} = \rho_{2n} - n, \tag{28}$$

where ρ_n and d_n are defined by Eqs. (23) and (24), respectively. There are three sets of unknowns (ρ_n, d_n, and ζ_n) constrained by two equations [Eqs. (23) and (24)]. The system is therefore not closed. It will be closed and the equations derived in this section will be solved below.

As an aside, for normal scaling with $\zeta_n = n\zeta$, this expression gives the Kolmogorov-like n-independent relation

$$\frac{\eta_n}{L} = \mathrm{Re}^{\frac{-1}{\zeta+1}}. \tag{29}$$

By requiring Eq. (29) to coincide with $\frac{\eta_2}{L} = \mathrm{Re}^{-3/4}$, we get the Kolmogorov result, $\zeta = 1/3$. Further, the so-called dissipative anomaly (or the zeroth law) [44] corresponds to $d_1 = 0$, which yields the result $\zeta_5 = 2\zeta_4 - 1$; from the point of view of the present theory, this result connecting ζ_4 and ζ_5 may be regarded just as basic as dissipative anomaly.

V. SCALING EXPONENTS TO ALL ORDERS

The quantitatively reasonable success of the simple statement $S_2(r) = (S_3(r))^{\frac{2}{3}} \propto r^{\frac{2}{3}}$ inspired many followers, both theorists and experimentalists, to assume that

$$S_{2n,0}(r) \equiv \langle (u(x+r) - u(x))^{2n} \rangle = A_{2n,0} r^{\zeta_{2n}} = A_{2n,0} r^{\frac{2n}{3}}, \tag{30}$$

where $A_{2n,0}$ could depend on large-scale properties. The closeness of the exponent to $2/3$ introduced Kolmogorov's energy spectrum $E(k) \propto \mathcal{P}^{\frac{2}{3}} k^{-\frac{5}{3}}$, dominating turbulence theory for many years. Data in hydrodynamic turbulence, plasma turbulence, and even in certain cosmological situations confirmed the approximate validity of this spectral form but considerable empirical work—for example, Ref. [28]—has shown that there are (modest) corrections to the $5/3$ exponent. Our goal is to *derive* not only the second-order exponent but exponents of all orders.

For that purpose, we use methods developed earlier [45–47] for the problem of a passive scalar advected by a random velocity field, generalized to the calculation of single-point probability density functions (PDFs) and moments of vorticity and dissipation rates in turbulence. Recently, a similar approach, combined with qualitative input from coherent structures, has been developed for the moments of velocity increments leading to quantitative derivation of anomalous scaling exponents [14,38]. Here, we improve on the past methods and derive an assumption-free quantitative expression for the exponents of structure functions to all orders, as well as for the moments of the dissipation rate in strong turbulence. We derive results explicitly for even orders but make comparisons also with negative moments for absolute values of velocity increments; the same principle should also apply to odd moments.

To derive structure functions $S_n(r)$ for $n \neq 3$, we need an expression for the pressure-velocity correlation function in Eq. (16) in the limit $\nu \to 0$. This places very strict constraints because of its nonlocality, which is the source of much complexity. We observe that the pressure contribution of Eq. (16) can only modify coefficients in the left-hand side, but it is clear that all powers other than 2 break the balance.

To close the Hopf equation, we have to calculate [see Eq. (16)]

$$\delta_r \frac{\partial p(x)}{\partial x} = \frac{\partial p(x+r)}{\partial (x+r)} - \frac{\partial p(x)}{\partial x}, \tag{31}$$

where $\delta_r p \sim \delta_r[\frac{\partial_i \partial_j}{\partial^2} u_i u_j]$. Since $r \gg \eta$, this relation involves two disparate length scales and is hard to deal with. Still, based on qualitative reasoning, coming from the Navier-Stokes equations, we have

$$\delta_r \nabla p = \delta_r \left[\nabla \frac{\nabla_i \nabla_j u_i u_j}{\nabla^2} \right] \approx \frac{1}{2} \frac{\partial (\delta_r u)^2}{\partial r} + O(v^2). \tag{32}$$

Now we present a dynamical derivation of this relation. To study the dynamics on the scales of interest $|x_1 - x_2| \approx r$, we have to eliminate the slowly varying, and known, velocity field at the large scale; in addition, contributions from the small-scale fluctuations in the interval $[\eta, r]$ have to be removed. We consider these two steps sequentially below.

As the Reynolds number increases, the slowly varying large-scale velocity field $\mathbf{u}_0(X)$ is first formed (see Ref. [15] and Sec. II); here X is the center of gravity coordinate $(x_1 + x_2)/2$. With further increase of the Reynolds number, a relatively high-frequency velocity fluctuations $\mathbf{v}$ develops, but the large-scale fluctuations $\mathbf{u_0}$ are stabilized by the effective viscosity (8), making them quasisteady. (In the literature on turbulence decay, this concept is often called permanence of large eddies.) Therefore, the equation for turbulent fluctuations in $\mathbf{u} = \mathbf{u_0} + \mathbf{v}$, where $\mathbf{v} = \mathbf{v}(\mathbf{k})$ with $k > \Lambda$, is derived in Ref. [15] to be

$$\partial_t \mathbf{v} + \mathbf{v} \cdot \nabla \mathbf{v} = -\nabla p + \mathbf{f} + \nu_0 \nabla^2 \mathbf{v}, \tag{33}$$

where ν_{tr} is the effective viscosity at the formation of the small-scale field $\mathbf{v}$ (cf. $\delta\nu$ in Sec. II). We then have

$$\mathbf{f} = -\mathbf{u}_0 \cdot \nabla \mathbf{v} - \mathbf{v} \cdot \nabla \mathbf{u_0} + (\nu_0 - \nu_{tr}) \nabla^2 \mathbf{u}_0. \tag{34}$$

In the local frame of reference X, we have

$$-\delta_r \mathbf{p_x}(\mathbf{X}, \mathbf{r}) = \delta_r \mathbf{v}_t + \delta_r \mathbf{v}(X, r) \partial_r \delta_r \mathbf{v}(X, r) = \delta_r \mathbf{v}_t + \frac{1}{2} \frac{\partial}{\partial r} (\delta_r \mathbf{v})^2. \tag{35}$$

In Eq. (16) what appears is the combination $\langle \delta_r(\partial_x p) \times (\delta_r u)^{2n-2} \rangle$. This can be obtained from the standard result on conditional expectations, which we apply below to the fluctuation field $\mathbf{v}$ as

$$\langle \delta_r \partial_x p(x) | (\delta_r v)^{2n-2} \rangle = \int_{-\infty}^{\infty} \left\langle \left[\delta_r v_t + \delta_r \partial_r \frac{1}{2} \delta v_r^2 \right] | (\delta_r v)^{2n-2} \right\rangle P(\delta_r v) d\delta_r v, \tag{36}$$

where P is the probability density function and we have not explicitly mentioned the dependence on r within the integral. It is in this way that we have removed the infrared fluctuations from the problem. Consequently, in the moving frame of reference, the slow, large-scale component disappears from the homogeneous equation of motion which becomes the equation for a flow in the inertial range of scales, $r > \eta$. In the early turbulence literature (e.g., see Ref. [48]), this approach, dealing with the infrared divergences, was called random Galilean transformation.

In addition to eliminating the slowly varying scales, we have to eliminate as the next step fluctuations from range $[\eta, r]$. This is achieved by using the smoothing procedure based on effective viscosity (8) which is the result of small-scale elimination (or coarse graining) in the interval $[r, \eta]$. In other words, it describes the effective viscosity acting on entities averaged over high-frequency

fluctuations in the interval $[r, \eta]$. Therefore, in the effective (coarse-grained) Navier-Stokes equations, the operator $\delta_r = \hat{x}$, where $\hat{x} \approx \delta_r$ stands for the coarse-grained local coordinate. As a result,

$$\frac{\partial u_r}{\partial t} + \frac{1}{2}\frac{\partial (u_r)^2}{\partial r} + O(v^2) = \frac{\partial}{\partial r}\nu_T(r)\frac{\partial}{\partial r}u_r - \frac{\partial p_r}{\partial r}, \tag{37}$$

where the turbulent viscosity $\nu_T(r) \approx r u_r \approx 0.085\frac{K^2}{\varepsilon} \approx 0.025(\delta_r u)^4/\varepsilon$, and $\delta_r u \equiv u_r$. The procedure leading to this equation is somewhat cumbersome but described in detail in Refs. [15,30].

As already mentioned, the basic idea of removing the infrared divergences using Lagrangian description with random Galilean transformation has been proposed for many years. But the major difference between those early efforts and the present is that the equations for the moments, with which we are dealing here, contain an infinite series of Wyld's diagrams coming from all orders of renormalized perturbation expansion, describing interactions of all orders. This feature is crucial, for, indeed, while large-scale fluctuations do "carry" small scales, they account only for a part of the dynamics involving coherent structures, and the origins of anomalous exponents cannot be unearthed from one-loop diagrams, or even an infinite set of them.

Thus, after removing fluctuations on length scales $l > r$ and $l < r$, we are left with the following equation, defined on an interval of size r for $p_r = p(r) - p(0)$ and $u_r = u(r) - u(0)$, averaged over positions in the flow:

$$\frac{\partial u_r}{\partial t} + \frac{1}{2}\frac{\partial u_r^2}{\partial r} + O(v^2) = \frac{\partial}{\partial r}\nu_T(r)\frac{\partial}{\partial r}u_r - \frac{\partial p_r}{\partial r}. \tag{38}$$

Here the $O(v^2)$ contribution includes $O(u_y\partial_y u_x)$. Substituting Eq. (38) into Eq. (16) gives a closed equation for structure functions as

$$\begin{aligned}\frac{\partial S_{2n,0}}{\partial r} + \frac{d-1}{r}S_{2n,0} - \frac{(d-1)(2n-1)}{r}S_{2n-2,2} \\ = -(2n-1)\left\langle\left[-\frac{\partial u_r}{\partial t} - \frac{1}{2}\partial_r u_r^2 + \partial_r \nu_T(r)\partial_r u_r + O(v^2)\right]\times u_r^{2n-2}\right\rangle,\end{aligned} \tag{39}$$

which is solved as below.

Since $\partial_t u_r \propto \partial_r u_r^2$ in the inertial range, we define $a = -\frac{\partial u_r}{\partial t} - \frac{1}{2}\partial_r u_r^2$ and take into account

$$a\frac{\partial(\delta u)^2}{\partial r}(\delta u)^{2n-2} = \frac{a}{n}\frac{\partial S_{2n}}{\partial r} \quad \text{and} \quad b = \langle(\delta v^2)(u_r)^{2n-2}\rangle \equiv S_{2n-2,2}, \tag{40}$$

as well as the relation based on Eqs. (8), namely, $\partial_r \nu_T(r)\partial_r u_r \approx 0.025\partial_r(u_r^2)$. From Eqs. (39) and (40) we finally obtain

$$\zeta_{2n,0} = \frac{(2n-1)(2-b)\frac{A_{2n-2,2}}{A_{2n,0}} - 2}{(1-2a)n + a}n. \tag{41}$$

It is to be stressed that a and b are not modeling constants but will be determined in the next section. This relation is subject to the constraint $a - b = \frac{1}{4}$ to guarantee that $\zeta_3 = 1$.

VI. THE ROLE OF TEMPORAL DERIVATIVES IN THE NAVIER-STOKES EQUATIONS

A. Steady state, $\frac{\partial u_r}{\partial t} = 0$: The Kolmogorov or normal scaling

The equation for the x component of nonlinearity in the Navier-Stokes equation (1) is given by

$$\partial_t u + \tfrac{1}{2}u^2 + u_y\partial_y u + u_z\partial_z u \approx \partial_t v_x + \tfrac{1}{2}\partial_x\left(v_x^2\right) + v_y\partial_y v_x + v_z\partial_z v_x + \partial_r \nu_T(r)\partial_r v_x + O(v^2). \tag{42}$$

By translational invariance small-scale elimination does not modify coefficients in front of convection terms but renormalizes the dissipation contribution by introducing $\nu_T(r)$ leading to Eq. (42) above.

The physics in Eqs. (39)–(42) describes the tendency to generate longitudinal sharp steps. The x-y and x-z terms prevent the shock formation by excitation of transverse y and z components of velocity field. This is manifested by the appearance of effective viscosity $\nu_T(r)$ in Eq. (38). From Eqs. (39) and (40) we readily obtain Eq. (41). As already mentioned, this relation is subject to the constraint $a - b = \frac{1}{4}$ to guarantee that $\zeta_3 = 1$. Neglecting the time derivative and turbulent viscosity in Eqs. (39)–(42) we obtain $a = \frac{1}{2}$ and $b = \frac{1}{4}$. Equation (41) simplifies to

$$\zeta_{2n,0} = \left[(2-b)(2n-1)\frac{A_{2n-2,2}}{A_{2n,0}} - 2\right]2n. \tag{43}$$

For Gaussian or "normal" (i.e., linear) scaling, $(2n-1)\frac{A_{2n-2,2}}{A_{2n,0}} = \zeta_0 = \text{const}$, so extrapolating the low-order relation $(2n-1)\frac{A_{2n-2,2}}{A_{2n,0}} = \frac{4}{3}$ into the large-n interval, one obtains Kolmogorov's exponents:

$$\zeta_{2n} = 2n/3, \qquad \zeta_3 = 1.$$

In the past, Kolmogorov's relations were mostly obtained from dimensional arguments, and the associated physics was contained in the so-called cascade models qualitatively describing the energy cascade from the large scale through the inertial range to small scales where it is dissipated into heat. No such process has been assumed in the above derivation.

B. Anomalous scaling and saturation of exponents

If we keep the time derivative in Eq. (38) and write out the turbulent viscosity just below Eq. (40), the numerical coefficients evaluated above change to $a = \frac{1}{2} - 0.025 = 0.475$ and $b = 0.225$ [from the constraint just below Eq. (41)]. The exponents $\zeta_{2n,0}$ are modified to

$$\zeta_{2n,0} = \frac{(\frac{9}{4} - a)(2n-1)\frac{A_{2n-2,2}}{A_{2n,0}} - 2}{(1-2a)n + a}n = \frac{0.366n}{0.05n + 0.475}. \tag{44}$$

The expression $(2n-1)A_{2n-2,2}/A_{2n,0} = 4/3$ for low moments; in fact, it is an approximate constant in the entire interval tested in numerical simulations. If this constancy holds in the limit $n \to \infty$, we are led to

$$\zeta_{2n} \to 7.3. \tag{45}$$

The physical meaning of saturation of exponents ζ_n in the limit $n \to \infty$ deserves special discussion. It follows from Eqs. (27) and (28) that, in this limit,

$$d_n \to \rho_n \to n \tag{46}$$

and

$$\langle(\varepsilon^n)\rangle \propto \left(\frac{r}{L}\right)^{d_n} = e^{n\ln(r/L)}, \tag{47}$$

resembling a gas of weakly interacting particles (logarithmic potential) confined in space. The implications of this result will be discussed in a future publication.

We point out that at low enough Reynolds numbers where Kolmogorov's 4/5 law has not yet been formed but falls short of the asymptotic value by a small logarithmic term, the exponents do not saturate but approach a constant logarithmically, but the qualitative effect is the same. The precise saturation value also depends on the value ascribed to $(2n-1)A_{2n-2,2}/A_{2n,0}$.

We will draw a few conclusions based only on the qualitative property that the saturation occurs. First, from Eq. (26), it readily follows that the smallest scale of turbulence applicable to large-order moments is given by

$$\eta_\infty = L\mathrm{Re}^{-1} = \eta\mathrm{Re}^{-1/4}, \tag{48}$$

which at high Reynolds numbers is much smaller than the Kolmogorov scale η. This has the important consequence that, as the Reynolds number increases, there is an increasing need to resolve DNS better and better—in the limit, up to η_∞, as was pointed out by Yakhot and Sreenivasan [49].

The second important conclusion is that the characteristic velocity fluctuation for very large n is given by

$$\left[\langle(\delta_r u)^{2n}\rangle/u_0^{2n}\right]^{1/2n} \propto (r/L)^{\zeta_{2n}/2n}. \tag{49}$$

When ζ_{2n} tends to a constant with increasing n, the right-hand side is unity, so it is clear that the velocity fluctuation over even the smallest scale can be of the order of the large-scale velocity u_0. This is an important practical consequence of anomalous exponents.

The result (48) has an implication for the singularities of the Navier-Stokes equations. In an interesting paper [50], the authors demonstrate that the weak solutions of the Navier-Stokes equations are regular, provided $d > 3/2$ in $\Lambda_c^* \propto \mathrm{Re}^{-3/(1+d)}$, where Λ_c^* is a parameter that demarcates the Euler-dominated large and inertial scales from the viscosity-dominated dissipation scales. For Kolmogorov [20], $d = 3$ and the solutions are clearly regular. The solutions are regular even for $d = 3/2$. According to us, $3/2$ is the smallest value that d assumes, thus ensuring the regularity of the weak solutions of the Navier-Stokes equations. (The theory uses constant ε but it is possible that one may need to account for the intermittency of ε [16].)

Another comment on the saturation of exponents ζ_{2n}, which resembles the situation for Burgers turbulence [51] with shocks, as well as passive scalars [51–53] is this: As already implied, there is always a competition between the effect of nonlinearity that tries to steepen fluctuations and pressure that tends to prevent it by distributing energy from one component to another, annulling the steepening effect of nonlinearity. It appears that for moments of high order, pressure is on the average incapable of countering the steepening effects, thus rendering the exponents of velocity increments to saturate (see Sec. III). Intermittency is the local (and instantaneous) imbalance between the two effects. Saturation is the sign of extreme intermittency when one of them, namely, the pressure effect, has become negligible.

One further implication of the saturation of exponents, keeping in mind Eq. (48), is that, for large n,

$$\eta_n \sim 1/\mathrm{Re} \sim 1/\varepsilon_{\max}. \tag{50}$$

VII. COMPARISONS WITH EXPERIMENTS AND SIMULATION

A. Anomalous scaling exponents

In this section, we make comparisons with a few aspects of the theory with experimental and simulations data. Table I shows the anomalous exponents ζ_n in the inertial range from the present theory (PT) as well as experiment (EXPT) and simulations (DNS). The experimental data are from time series using Taylor's hypothesis (i.e., the time increment δt in turbulence being advected by a mean flow U is equivalent to the spatial increment, $r = \delta t \times U$). The numbers are obtained by choosing the inertial range to be the one within which the third-order structure function has an acceptably good linear region, according to the $4/5$ law. We also list the data from the extended self-similarity (ESS) analysis of Benzi *et al.* [23]. Below that row, we show scaling of structure functions with actual spatial separation (i.e., with no use of Taylor's hypothesis) from simulations on a large 8192^3 grid [27]. Finally, comparisons are made also with the geometric model by She and Leveque [54]. It is clear that the theory is in excellent agreement with the data. The data correspond to $n > 1$ (see Table II for $n < 1$). We show the comparison graphically (Fig. 1) between the theory and various data sources listed in the table. We also add an inset which plots ζ_n/n versus $1/n$ to show the asymptotic saturation behavior for large n. Saturation is plausible even though the approach appears to be slow. No experiment or simulation has shown this saturation compellingly for longitudinal structure functions, but it is clear that they are in agreement with the theory in the

TABLE I. Scaling exponents ζ_n of velocity structure functions $S_n \propto r^{\zeta_n}$. The rows in order are as follows: PT, present theory; EXPT, experiment from Ref. [24], using Taylor's hypothesis; ESS, exponents for similar data measured using the extended self-similarity [23]; DNS, spatial data from large-scale direct numerical simulations on an 8192^3 grid; ER, error bars on both sides of the mean values from DNS in the row above, rounded off to the lowest integer level; and SL, geometric model of Ref. [54].

n	1	2	3	4	5	6	7	8	9	10	11	12	13	14
PT	0.366	0.7	1.0	1.27	1.525	1.76	1.97	2.17	2.35	2.52	2.68	2.83	2.97	3.1
EXPT		0.7	1.0	1.25	1.56	1.8	2.0	2.2	2.3	2.5				
ESS		0.7	1.0	1.28	1.53	1.77	2.01	2.23						
DNS		0.7	1.0	1.32	1.56	1.81	2.02	2.21	2.38	2.52	2.66	2.74		
ER		3×10^{-3}	10^{-2}	4×10^{-3}	10^{-2}	7×10^{-3}	2×10^{-2}	10^{-2}	5×10^{-2}	3×10^{-2}	4×10^{-2}	4×10^{-2}		
SL	0.36	0.70	1.0	1.28	1.54	1.78	2.00	2.21	2.41	2.6	2.8	2.9	3.1	3.25

range of overlap. It must be noted that transverse structure functions are known to display saturation beyond $n = O(10)$ (see Ref. [28]).

In Table II, we list the exponents measured for low-order structure functions with absolute values. The experimental data are from Ref. [25] and the DNS data are from Ref. [26]. The agreement with the theory (as well as between experiment and simulations) is remarkable.

The next items to compare are the exponents ρ_n and d_n (Table III). From the computation of the inertial range exponents ζ_n, one can compute the exponents ρ_n and d_n, using formulas (27) and (28). In experiment and simulations, these two quantities were determined independent of the ζ_n from Table I, and therefore the comparison with the theory is to be regarded as having an independent value. Considering the complexity of the measurements, the agreement can be regarded as excellent.

B. Large-scale Gaussian state in fully developed turbulence

Gaussianity is a valid result for wavenumbers that are small compared to the forcing wavenumber, or for length scales that are large compared to the forcing length scale. In practice, this seems to work very well for scales of the order of the integral scale. From well-resolved DNS studies of homogeneous and isotropic turbulence presented in Ref. [28], in the largest simulations in boxes of 8192^3, we compare below the actual moments of velocity differences. The original paper should be

TABLE II. Comparison of scaling exponents from the present theory with those from experiments [25] and DNS data [26]. For all orders used here (including the two negative n values), we have used the absolute values of the structure functions.

n	DNS exponents	Experiment	Present theory
1	0.366	0.372	0.366
0.9	0.332	0.333	0.331
0.8	0.296	0.292	0.296
0.7	0.260	0.265	0.260
0.6	0.223	0.221	0.224
0.5	0.187	0.190	0.187
0.4	0.150	0.150	0.151
0.3	0.112	0.113	0.114
0.2	0.073	0.076	0.076
0.1	0.036	0.039	0.028
−0.2	−0.077	0.078	−0.028
−0.8	−0.317	−0.313	−0.321

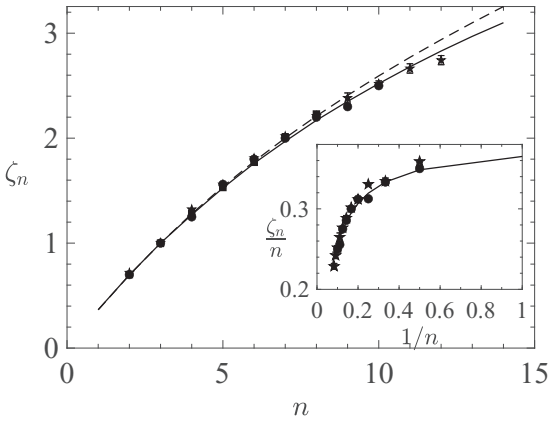

FIG. 1. Comparison of theoretical predictions (44) for the anomalous exponents ζ_n with experimental and simulations data. Where the error bars are not visible in experimental and simulations data, they are smaller than the symbol size. The present theory is indicated by the solid line, and the She-Leveque theory by the dashed line. The inset shows the ratio ζ_n/n plotted against $1/n$. It is clear that the saturation tendency is visible in both the theory and experiment as well as simulations.

consulted for issues on resolution and convergence. The numbers are presented in groups of three as (order of moment $2n$, DNS moments, theoretical moments for the Gaussian), the last one being simply $(2n-1)!!$. The numbers are (4, 2.98, 3), (6, 14.9, 15), (8, 105.3, 105), (10, 957.2, 945), (12, 10906.5, 10395), and (214, 169208, 135135). Except for $2n = 14$, amazingly, they are within a few percent of the theoretical values.

The situation appears satisfactory even in a turbulent boundary layer in the fully turbulent part where the effects of outer intermittency are not strong. A similar comparison yields the following result [55]: (4, 2.83, 3), (6, 14.75, 15), (8, 108.1, 105), (10, 1039, 945), and (12, 13322, 135135). Even though the flow is not homogeneous and isotropic, it is astonishing that large scales of the order L are closely Gaussian. The generality of this result may be due to the central limit theorem, which is always valid if there are weakly interacting particles or waves, as in an ideal gas [40]. With increase of "particle concentration," it becomes unstable and becomes nonlinear and/or intermittent.

Though less extensive, the available evidence in a very high Reynolds number atmospheric boundary layer is also supportive. In Ref. [56], for an atmospheric boundary layer at a height of 2 m, corresponding to a microscale Reynolds number of about 5869, the fourth- and sixth-order structure functions $S_{2n}(r)$ for large r of the order L were found to be 2.9 and 15.2, respectively, very close to $(2n-1)!!$. In an independent but similar measurement at about 30 m above the ground [56], for which $R_\lambda = 10340$, the corresponding result for $2n = 6$ was 15. (Higher-order data at these high Reynolds numbers are unavailable because of convergence issues.)

TABLE III. Comparison of derived exponents d_n and d_n with outcomes of DNS and experimental data. Theory: expressions (27), (28), and (44); DNS data from Ref. [42]. Experiment from Ref. [24].

	ρ_n			d_n		
n	Theory	DNS	Experiment	Theory	DNS	Experiment
1	0.465	0.463	0.455	0	0	0
2	1	1	1	0.17	0.145	0.18
3	1.55	1.579	1.478	0.49	0.44	0.56 ± 0.06
4	2.17	2.187	2.05	0.93	0.884	0.96 ± 0.15
5	2.83	2.817	2.66 ± 0.14	1.4	1.467	
7	4.241	4.128	3.99 ± 0.65			

We thus conclude that in fully turbulent parts of turbulent shear flows, except for very close to the wall, the large-scale fluctuations are not far from Gaussian. We believe it is this feature of the large scales in a broad range of circumstances that enables low-order engineering models to work well (see, for example, Refs. [10,11,14]). It appears that the large scales are closely Gaussian for conditions (5) and (6) obtained in the weak-coupling limit, for which the result is asymptotically exact and can be used as the basis for accurate evaluations of various constants in the inertial range. It also appears to be the case for naturally created shear flows, at least when the Reynolds numbers are very large.

C. Transition to the inertial range

We showed in Secs. II and III that the Taylor microscale Reynolds number in the inertial range, based on an effective viscosity which has been computed from renormalization group methods, assumes a universal value of about 8.8. As long as the global Reynolds number is large enough to sustain turbulence, the inertial range maintains itself at that Reynolds number. A qualitative point supporting this universality is the demonstration by Townsend [57] that the Reynolds number based on an eddy viscosity is 12.5 for turbulent wakes. He discussed the result in the following physical terms (as interpreted by us). A turbulent flow is essentially on the verge of instability which waxes and wanes in time. At some point in the cycle, the "mean flow" undergoes a transition at a certain critical Reynolds number. The fluctuations then extract energy from the mean flow, thus increasing the effective viscosity and reducing the Reynolds number, thus stabilizing the flow. The finite amplitude fluctuations in this newly stabilized flow grow with time and the flow becomes unstable again, and the cycle continues. Using the standard relation between the definitions of the Reynolds numbers, this number reduces to a microscale Reynolds number of order 10. This scenario applies to other flows such as jets. Townsend loosely saw this mechanism as the source of large structure in a shear flow. This idea has been developed more explicitly for mixing layers, wakes, and boundary layers in Ref. [58].

But when does turbulence originate? A complementary part of our contention is that if we start with a cleanly prepared Gaussian state, the transition to the anomalous scaling range ensues when the ordinary microscale Reynolds number based on fluid viscosity exceeds the same critical value of 9. This is demonstrated in the process of transition to turbulence as one increases the Reynolds numbers of Gaussianly forced box turbulence [41,42,59]. The left panel of Fig. 2 shows the predictions are supported well by high-quality DNSs in homogeneous and isotropic turbulence. Essentially, these simulations show that the derivative moments M_n, which satisfy the Gaussian relation $M_n = (2n-1)!!$ for $2 \leqslant n \leqslant 6$ for $R_{(\lambda,T)} = \mathrm{Re}^* \approx 9$ begin to rise and follow power laws of the type $M_n = A_n \mathrm{Re}^{d_n}$, with well-defined exponents d_n given by Eq. (44). The top left figure shows the moments of velocity derivatives, $M_n = \langle(\partial_x u)^n\rangle/(M_2)^n$. The transition to the anomalous multiscaling region occurs at $R_\lambda \approx 9$. An interesting feature is the Reynolds number dependence of the transition with the moment order $2n$ (see right-hand panel of Fig. 2). This nontrivial effect is readily explained by the decrease of the volume fraction of the flow occupied by increasingly rarer events [16]; see also Ref. [42]. A change in velocity gradient structure observed by Ref. [60] is also consistent with this picture.

Finally, as the Reynolds number of the flow increases past the transition points, the exponents d_n can be seen in Fig. 3 to agree with the theoretical result quite well. We have provided only the best fits to the data and not assigned any formal error bars, which would seem unnecessary at this point of development of the idea.

A further supporting evidence comes from channel flow and thermal convection studies [59,61,62], though the picture in these two latter flows is somewhat complex. In Ref. [61], the authors concluded as follows: "For small Reynolds numbers … a transition occurs from sub-Gaussian or nearly Gaussian velocity gradient statistics to intermittent non-Gaussian ones. At the transition Reynolds number the derivative fluctuations are Gaussian."

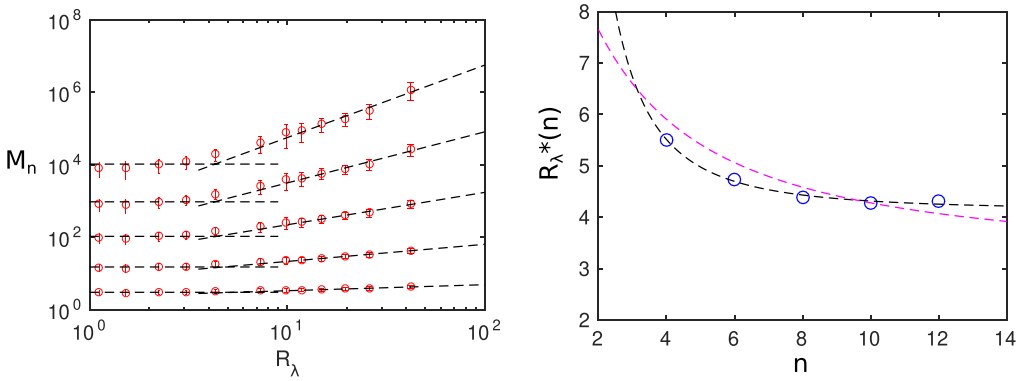

FIG. 2. Left: Normalized moments of velocity gradients, M_n, for $n = 2, 3, 4, 5$, and 6, from direct numerical simulations of the Navier-Stokes equations [41,42]. For low Reynolds numbers, each of the moments is given by $(2n-1)!!$; i.e., they obey Gaussian statistics, as shown by horizontal lines. Each moment takes off, almost abruptly, to follow the fully developed anomalous scaling relations given by the theory, Eq. (23). The lowest moment undergoes a transition from a Gaussian to an anomalous state at a Reynolds number of about 9. Higher moments undergo this transition at lower Reynolds numbers $R_\lambda^*(n)$, for which sub-Gaussian fluctuations reflecting a more complex dynamics of forcing are responsible. These Reynolds numbers are shown on the right panel, where theory (dashed line through the circles) and simulations (the second dashed line) are compared. We do not deal with this particular aspect of the theory in this paper but refer the reader to Refs. [41,42].

We point out that the initially Gaussian state does not preclude the presence of organized structures. The evidence below is worth recalling though it should be regarded as suggestive. Flows lose their stability in successive stages, and develop structures, before eventually succumbing to transition. However, the transition to turbulence is not a consequence of successive loss of stability but an abrupt phenomenon, qualitatively resembling the abrupt appearance of the onset of temporal chaos [63]. Our theory does not address the generation of well-organized transitional structures, however interesting and important they are in their own right. We recall Busse's [64] remark that at moderate Prandtl numbers, turbulent convective large structures fluctuate in both space and time, despite their well-organized orientation. He remarked that this state combines random processes with the permanence of a large-scale organizing structure. In other words, the initial Gaussian

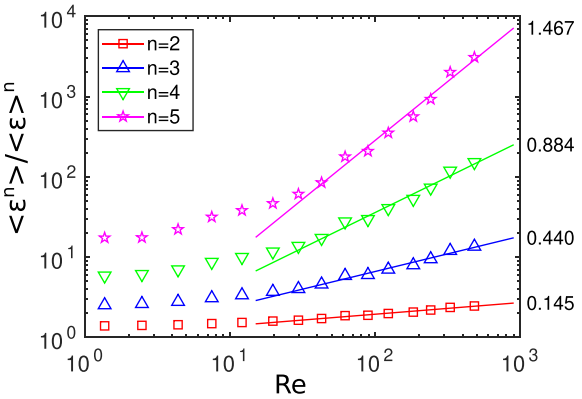

FIG. 3. Comparison of theoretical predictions for the exponents d_n through the transitional region with numerical simulations of Refs. [41,42]. The numbers to the right are least-squares experimental fits to the power-law regions. Table II provides comparisons of the exponents.

state encompasses all possible structures, and the transition takes place when R_λ exceeds about 9, this being the last stage of breakdown. In the specific example of the boundary layer, we are not concerned with the generation of well-organized structures such as the Tollmien-Schlichting waves, the development of three-dimensional structure, the formation of axial vortices, etc., but with the eventual breakdown of the flow; even the precise form of this breakdown does not appear explicitly in our considerations. To give an example, in the boundary layer the scenario one might surmise is the breakdown of the flow to form turbulent spots, as described by Narasimha [65]; see also Ref. [66]. Our stipulations are that (1) the state prior to the breakdown is essentially Gaussian, and that (2) the breakdown itself happens independently of the formation of the instability structures abruptly at an R_λ of about 9. As another anecdotal evidence, we note the demonstration in Ref. [66] that the velocity perturbation in the form of an axial vortex embedded in a boundary layer undergoes inflectional instability at a vortex Reynolds number of 10.

The final picture is the following. The slowly varying large-scale flow is closely Gaussian. If it is prepared to possess no fluctuations and the forcing is Gaussian, it undergoes a transition to turbulence at a microscale Reynolds number, using normal viscosity, of about 9. This statement applies even in the presence of organized structures. In practice, this Reynolds number could exceed the critical value by manyfold. Under these conditions, the inertial range that develops has two properties: (1) its effective microscale Reynolds number is always about 8.8 when based on effective viscosity, a result derived from the RG methods; and (2) the inertial range possesses anomalous exponents, which we have been able to calculate with no *ad hoc* modeling.

VIII. DISCUSSION AND CONCLUSIONS

It this paper we have developed a novel approach for closing the Hopf equations leading to the determination of anomalous exponents in three-dimensional turbulence. For almost 50 years this problem had eluded researchers in the field and was relegated to the list of "unsolved problems." Very close agreement of the calculated multiscaling exponents of structure functions and moments of derivatives with experimental data justifies the details of the theory. We note that no uncontrolled models have been used and hope that this effort will contribute to discussion of whether, at long last, we have the essential elements in place for the elusive theory of turbulence, for the specific aspects considered here.

To reiterate, we considered the Navier-Stokes equations for an infinite fluid driven at a fixed wavenumber Λ, and discussed the two physically different intervals: the infrared limit $k \ll \Lambda$ and the ultraviolet limit $k \gg \Lambda$ overlapped at the energy forcing scale $k = \Lambda$ corresponding to the universal Reynolds number, $R_\lambda = R_\lambda^T \approx 9$. We further showed that the ranges $k \ll \Lambda$ and $k \gg \Lambda$ correspond to "equilibrium" and inertial ranges of fully developed turbulence, respectively. Therefore, the forcing scale Λ stands for the integral scale of turbulence and, simultaneously, for the mean free path of an equilibrium system. Depending on the Reynolds number R_λ, the flow can be in either regime. This Reynolds number marks the transition point from the Gaussian to the multiscaling behavior of strong (ultraviolet) turbulence.

In the inertial range, where viscous effects are zero, the effective or turbulent viscosity ν_T, characterizing the energy flux from large to small scales, is length-scale independent, equal to $R_\lambda^T \approx 8.8 = \text{const}$, independent of both the"bare" viscosity and the forcing power. Since, asymptotically, the Gaussian infrared range can be calculated to all orders in a perturbation expansion, the continuous transition at $R_\lambda^T \approx 8.8$ means that the entire ultraviolet interval and inertial range are accurately represented by expressions (8). We have presented available evidence in both the infrared and the ultraviolet regions to support the theoretical results.

We wish to stress a few essential points.

(1) No experimentally adjustable parameters were involved in the calculations. Representation of dissipation processes in terms of point splitting, connecting dissipation, and inertial range dynamics, based on the natural assumption $\partial_x u \approx \frac{\delta_\eta u}{\eta}$ of the analyticity of velocity field in the dissipation range, is a well-accepted and understood procedure. Also, at the transition point, the

universal and scale-independent Reynolds number $R_\lambda \approx 9$ provided an additional numerical support for our calculations.

(2) We dealt explicitly with the correlation of the pressure gradient and velocity increment in the inertial range scale r. According to Landau and Lifshitz [40] the effective viscosity on this scale is $\nu_T \approx r(u(x+r) - u(x) = r\delta_r u$. This natural expression appears in the Navier-Stokes equations as a result of scale elimination from the interval $[\eta, r]$. As a result, in the coarse-grained NS equations, the spatial coordinate $\hat{x} = \delta_r x$ enabled us to evaluate $\delta_r \partial_x p$ and close the Hopf equations for the moment-generating function of the velocity field. The matching conditions on dissipation and integral scales provided the relations needed for closure of the Hopf equations. This led to explicit expressions for structure functions in the inertial range and moments of derivatives related to dissipation scales. The anomalous exponents ζ_n coming from the derived equations agreed with experimental and numerical data in the entire range $-1 < n$. (For negative n, we take absolute values of the velocity increments.) Again, no adjustable parameter was involved in the calculation; the only coefficients needed in the theoretical expressions, namely, a and b, were obtained from the Navier-Stokes equations and from the theoretically valid constraint $S_3 = 1$, respectively.

(3) Perhaps surprisingly, neglecting the time derivative in the equation for the pressure gradient resulted in the expression for the normal Kolmogorov scaling $\zeta_{2n} = 2n/3$. Accounting for the contribution of the time derivative turned out to be crucial.

(4) We found that in the limit $n \to \infty$ the exponents ζ_{2n} saturate, resembling the situation in the compressible case of Burgers turbulence as well as passive scalars, both of which contain no pressure. The saturation suggests that the pressure effects are substantially diminished for high-order structure functions.

(5) Finally, we argued that the transition from the Gaussian to multiscaling state is effectively no different from the laminar-turbulent transition and supported it by invoking a number of simulations. This result has now been demonstrated very convincingly for homogeneous and isotropic turbulence for different types of forcing and for two types of flows [41,42,59,61], in which the Gaussian state transitions to the multiscaling at $R_\lambda^* \approx 9$ as well.

All these results bring us to ask ourselves if we have the right ingredients of the theory for turbulence in the context of large-scale behavior as well as the scaling exponents. The all-encompassing theory of turbulence may be elusive because some properties of turbulence will depend on specifics of initial and boundary conditions, but the essential ingredients of the theory for scales participating in the energetic dynamics appear to be on hand. We have also argued that some specific results are applicable to a variety of other flows as well—so we ask (with humility) whether we are approaching the solution to the anomalous scaling problem in turbulence theory.

ACKNOWLEDGMENTS

This paper is the result of some 25 years of collaboration between the two authors. Over this time, we have discussed our work with many colleagues too numerous to list here, and are grateful to all of them. We should particularly acknowledge the early influence of the late S. Orszag, and numerous discussions over the years with H. Chen, D. A. Donzis, G. L. Eyink, K. P. Iyer, S. Khurshid, A. M. Polyakov, J. Schumacher, L. Smith, and I. Starosel'sky.

[1] L. Euler, Principes généraux du mouvement des fluides [The general principles of the movement of fluids], Mem. Acad. Sci. Berlin **11**, 274 (1757).

[2] M. Navier, Mémoire sur les lois du mouvement des fluides [Memorandum on the laws of motion of fluids], Mem. Acad. Sci. **6**, 389 (1827).

[3] G. G. Stokes, On the theories of internal friction of fluids in motion, Trans. Cambridge Philos. Soc. **8**, 287 (1845).

[4] O. Reynolds, On the dynamical theory of incompressible viscous fluids and the determination of the criterion, Philos. Trans. R. Soc. London **186**, 123 (1894).
[5] H. W. Wyld, Formulation of theory of turbulence in an incompressible fluid, Ann. Phys. **14**, 143 (1961).
[6] A. S. Monin and A. M. Yaglom, *Statistical Fluid Mechanics: Mechanics of Turbulence* (MIT Press, Cambridge, MA, 1975), Vol. II.
[7] R. H. Kraichnan, The structure of isotropic turbulence at very high Reynolds number, J. Fluid. Mech. **5**, 497 (1959).
[8] R. H. Kraichnan, Lagrangian history closure approximation for turbulence, Phys. Fluids **8**, 575 (1965).
[9] S. A. Orszag and M. D. Kruskal, Theory of Turbulence, Phys. Rev. Let. **16**, 441 (1966).
[10] B. E. Launder and D. B. Spalding, *Mathematical Models of Turbulence* (Academic Press, New York, 1972).
[11] B. E. Launder and D. B. Spalding, The numerical computation of turbulent flows, Comput. Methods Appl. Mech. Eng. **3**, 269 (1974).
[12] V. Yakhot and S. A. Orszag, Renormalization analysis of turbulence. I. Basic theory, J. Sci. Comput. **1**, 3 (1986).
[13] V. Yakhot, S. A. Orszag, T. Gatski, S. Thangam, and C. Speciale, Development of turbulence models for shear flows by a double expansion technique, Phys. Fluids A **4**, 1510 (1992).
[14] C. Bartlett, H. Chen, I. Staroselsky, J. Wanderer, and V. Yakhot, Lattice Boltzmann two-equation model for turbulence simulations: High-Reynolds number flow past circular cylinder, Int. J. Heat Fluid Flow **42**, 1 (2013).
[15] V. Yakhot, Reynolds number of transition and self-organized criticality of strong turbulence, Phys. Rev. E **90**, 043019 (2014).
[16] K. R. Sreenivasan and C. Meneveau, Singularities of the equations of fluid motion, Phys. Rev. A **38**, 6287 (1988).
[17] C. Domb and M. S. Green, *Phase Transitions and Critical Phenomena* (Academic Press, New York, 1976).
[18] M. Creutz, P. Mitra, and K. J. M. Moriarty, Computer investigations of the three-dimensional Ising model, J. Stat. Phys. **42**, 823 (1986).
[19] L. Onsager, The distribution of energy in turbulence, Phys. Rev. **68**, 286 (1945).
[20] A. N. Kolmogorov, The local structure of turbulence in incompressible viscous fluid for very large Reynolds number, Dokl. Akad. Nauk SSSR **30**, 9 (1941).
[21] A. Polyakov, A similarity hypothesis in the strong interactions. I. Multiple hadron production in e^+e^- annihilation, Sov. Phys. JETP **32**, 296 (1971).
[22] F. Anselmet, Y. Gagne, E. J. Hopfinger, and R. A. Antonia High-order velocity structure functions in turbulent shear flows, J. Fluid Mech. **140**, 63 (1984).
[23] R. Benzi, S. Ciliberto, C. Baudet, and G. R. Chavarria, On the scaling of three dimensional homogeneous and isotropic turbulence, Physica D **80**, 385 (1995).
[24] K. R. Sreenivasan and R. A. Antonia, The phenomenology of small-scale turbulence, Annu. Rev. Fluid Mech. **29**, 435 (1997).
[25] K. R. Sreenivasan and B. Dhruva, Is there scaling in high-Reynolds-number turbulence? Prog. Theor. Phys. Suppl. **130**, 103 (1998).
[26] S. Y. Chen, B. Dhruva, S. Kurien, K. R. Sreenivasan, and M. A. Taylor, Anomalous scaling of low-order structure functions of turbulent velocity, J. Fluid Mech. **533**, 183 (2005).
[27] K. P. Iyer, K. R. Sreenivasan, and P. K. Yeung, Reynolds number scaling of velocity increments in isotropic turbulence, Phys. Rev. E **95**, 021101(R) (2017).
[28] K. P. Iyer, K. R. Sreenivasan, and P. K. Yeung, Scaling exponents saturate in three-dimensional isotropic turbulence, Phys. Rev. Fluids **5**, 054605 (2020).
[29] D. Forster, D. Nelson, and M. J. Stephen, Large-distance and long-time properties of a randomly stirred fluid, Phys. Rev. A **16**, 732 (1977).
[30] V. Yakhot and L. Smith, The renormalization group, the ϵ-expansion and derivation of turbulence models, J. Sci. Comput. **7**, 35 (1992).
[31] E. Hopf, Statistical hydrodynamics and functional calculus, J. Rat. Mech. Anal. **1**, 87 (1952).
[32] A. M. Polyakov, Turbulence without pressure, Phys. Rev. E **52**, 6183 (1995).

[33] V. Yakhot, Mean-field approximation and a small parameter in turbulence theory, Phys. Rev. E **63**, 026307 (2001).
[34] R. J. Hill, Equations relating the structure functions of all orders, J. Fluid Mech. **434**, 379 (2001).
[35] V. Yakhot, Pressure-velocity correlations and scaling exponents in turbulence, J. Fluid Mech. **495**, 135 (2003).
[36] V. Yakhot, Probability density and scaling exponents of the moments of longitudinal velocity difference in strong turbulence, Phys. Rev. E **57**, 1737 (1998).
[37] S. Kurien and K. R. Sreenivasan, Anisotropic scaling contributions to high-order structure functions in high-Reynolds-number turbulence, Phys. Rev. E **62**, 2206 (2000).
[38] T. Gotoh and T. Nakano, Role of pressure in turbulence, J. Stat. Phys. **113**, 855 (2003).
[39] C. De Dominicis and P. C. Martin, Energy spectra of certain randomly-stirred fluids, Phys. Rev. A **19**, 419 (1979).
[40] L. D. Landau and E. M. Lifshitz, *Fluid Mechanics* (Pergamon, New York, 1982).
[41] V. Yakhot and D. A. Donzis, Emergence of Multiscaling in a Random-Force Stirred Fluid, Phys. Rev. Lett. **119**, 044501 (2017).
[42] V. Yakhot and D. A. Donzis, Anomalous exponents in strong turbulence, Physica D **384**, 12 (2018).
[43] A. N. Kolmogorov, Energy dissipation in locally isotropic turbulence, Dokl. Akad. Nauk SSSR **32**, 19 (1941).
[44] K. R. Sreenivasan, The scaling of the energy dissipation rate, Phys. Fluids **27**, 1048 (1984).
[45] Y. G. Sinai and V. Yakhot, Limiting Probability Densities of a Passive Scalar in a Random Velocity Field, Phys. Rev. Lett. **63**, 1962 (1989).
[46] V. Yakhot and A. Cheklov, Algebraic Tails of Probability Density Functions in the Random-Force-Driven Burgers Turbulence, Phys. Rev. Lett. **77**, 3118 (1996).
[47] V. Yakhot, Passive scalar advected by a rapidly changing velocity field: Probability density of scalar differences, Phys. Rev. E **55**, 329 (1997).
[48] B. B. Kadomtsev and V. I. Petviashvili, On the stability of solitary waves in weakly dispersive media, Sov. Phys. Dokl. **15**, 539 (1970).
[49] V. Yakhot and K. R. Sreenivasan, Anomalous scaling of structure functions and dynamic constraints on turbulence simulations, J. Stat. Phys. **121**, 823 (2005).
[50] A. Cheskidov and R. Shvydkoy, A unified approach to regularity problems for the 3D Navier-Stokes and Euler equations: The use of Kolmogorov's dissipation range, J. Math. Fluid Mech. **16**, 263 (2014).
[51] J. Bec and K. Khanin, Burgers turbulence, Phys. Rep. **447**, 1 (2007).
[52] R. H. Kraichnan, Anomalous Scaling of a Randomly Advected Passive Scalar, Phys. Rev. Lett. **72**, 1016 (1994).
[53] A. Celani, A. Lanotte, A. Mazzino, and M. Vergassola, Universality and Saturation of Intermittency in Passive Scalar Turbulence, Phys. Rev. Lett. **84**, 2385 (2000).
[54] Z.-S. She and E. Leveque, Universal Scaling Laws in Fully Developed Turbulence, Phys. Rev. Lett. **72**, 336 (1994).
[55] L. Zubair, Studies in turbulence using wavelet transforms for data compression and scale separation, Ph.D. thesis, Yale University, 1993.
[56] B. Dhruva, An experimental study of high Reynolds number turbulence in the atmosphere, Ph.D. thesis, Yale University, 2000.
[57] A. A. Townsend, *The Structure of Turbulent Shear Flow* (Cambridge University Press, Cambridge, UK, 1956).
[58] K. R. Sreenivasan, A unified view of the origin and morphology of the turbulent boundary layer structure, in *Turbulence Management and Relaminarisation*, edited by H. W. Liepmann and R. Narasimha (Springer-Verlag, Berlin, 1988), pp. 37–61.
[59] J. Schumacher, K. R. Sreenivasan, and V. Yakhot, Asymptotic exponents from low-Reynolds-number flows, New J. Phys. **9**, 89 (2007).
[60] R. Das and S. S. Girimaji, On the Reynolds number dependence of velocity-gradient structure and dynamics, J. Fluid Mech. **861**, 163 (2019).

[61] J. Schumacher, J. D. Scheel, D. Krasnov, D. A. Donzis, V. Yakhot, and K. R. Sreenivasan, Small-scale universality in fluid turbulence, Proc. Natl. Acad. Sci. USA **111**, 10961 (2014).
[62] J. Schumacher, A. Pandey, V. Yakhot, and K. R. Sreenivasan, Transition to turbulence scaling in Rayleigh-Bénard convection, Phys. Rev. E **98**, 033120 (2018).
[63] D. Ruelle and F. Takens, On the nature of turbulence, Commun. Math. Phys. **20**, 167 (1971).
[64] F. H. Busse, Non-linear properties of thermal convection, Rep. Prog. Phys. **41**, 1929 (1978).
[65] S. Dhawan and R. Narasimha, Some properties of boundary layer flow during the transition from laminar to turbulent motion, J. Fluid Mech. **3**, 418 (1958).
[66] C. F. Pearson and F. H. Abernathy, Evolution of the flow field associated with a streamwise diffusing vortex, J. Fluid Mech. **146**, 271 (1984).